The following Communications have been judged by at least two referees to be "very important papers" and are published online at www.angewandte.org:

Books

Highlights

C–C Coupling

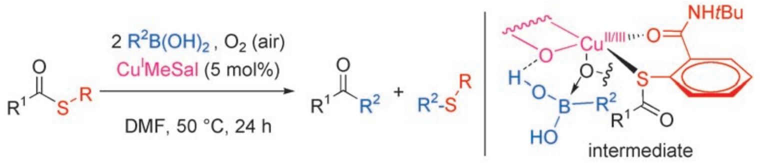

Getting rid of palladium: Thiol esters can be cross-coupled with boronic acids to generate ketones at neutral pH by using a Cu^I-oxygenate catalyst under aerobic and Pd-free conditions (see scheme; S-pendant = NH*t*Bu thiosalicyclamide). The mechanistically unique coupling is likely to proceed by a preorganized, higher oxidation state Cu species that relies on appropriately positioned ligating S-pendant groups on the thiol ester and on an additional equivalent of the boronic acid.

Asymmetric Epoxidation

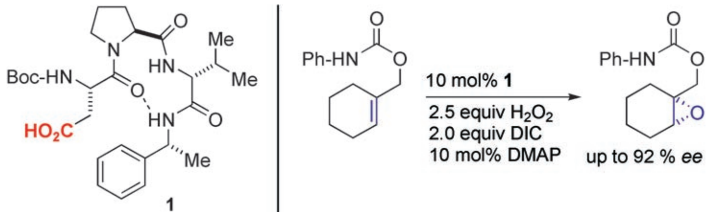

Oxidation per carboxylic acid: Upon incorporation into a suitable tripeptide, per-aspartate can epoxidize olefins that contain hydrogen-bonding groups with high enantioselectivity (up to 92% *ee*). Catalytic asymmetric epoxidation can be effected with hydrogen peroxide as the terminal oxidant and carbodiimide as the stoichiometric activator for multiple acid/peracid turnovers.

Correspondence

Crystal Growth (1)

Symmetry violation: Recent results by Tremel and co-workers on the phase selection of calcium carbonate through the chirality of adsorbed amino acids appear to provide a deterministic route to “mirror-symmetry breaking”, which may have ramifications for the emergence of homochirality on Earth. In our view, however, the crystallization experiments violate basic rules of symmetry and we suspect the presence of chemical, biological, or other homochiral or achiral contaminants in the system.

Crystal Growth (2)

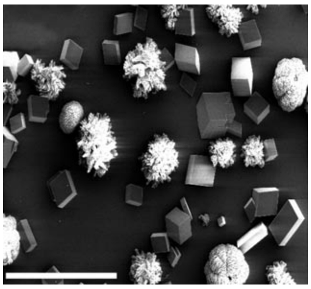

Like chalk and cheese: Although the model put forward by Lahav and Leiserowitz may be quite reasonable for the crystallization of glycine in the presence of amino acids, it is not the case for the crystallization of $CaCO_3$ (see picture). In the latter case, the amino acids present cannot be considered to be innocent molecules as they are involved as ligands in the coordination chemistry of Ca^{2+}. New results indicate that homochiral impurities are not the driving force for the phase selection: When added intentionally, they annihilate the observed phase selectivity rather than promote it.

Minireviews

Acyltransferases

The low specificity of bacterial acyltransferases is utilized in the development of numerous biotechnology processes for lipid modification, a field that is dominated by the use of lipases. In contrast to lipases, these reactions are catalyzed in vivo in whole-cell fermentations. Thus wax esters, thio wax esters, or fatty-acid ethyl esters, a possible substitute for biodiesel, can be derived directly from renewable resources.

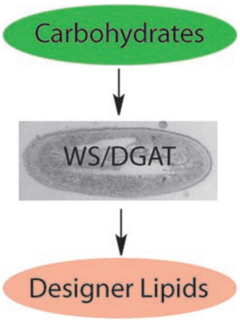

For the USA and Canada: ANGEWANDTE CHEMIE International Edition (ISSN 1433-7851) is published weekly by Wiley-VCH, PO Box 191161, 69451 Weinheim, Germany. Air freight and mailing in the USA by Publications Expediting Inc., 200 Meacham Ave., Elmont, NY 11003. Periodicals postage paid at Jamaica, NY 11431. US POSTMASTER: send address changes to *Angewandte Chemie*, Wiley-VCH, 111 River Street, Hoboken, NJ 07030. Annual subscription price for institutions: US$ 7225/6568 (valid for print and electronic / print or electronic delivery); for individuals who are personal members of a national chemical society prices are available on request. Postage and handling charges included. All prices are subject to local VAT/sales tax.

Reviews

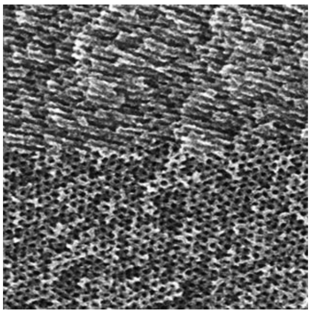

The right combination of new techniques, which use a large variety of hard and soft templates in the controlled synthesis of mesoporous carbon materials with well-defined nanostructures, and surface modification of these materials offers new perspectives for carbon material applications. The picture shows a high-resolution view of the surface structure of a fibrous material formed from phloroglucinol.

Nanostructured Carbon

C. Liang, Z. Li, S. Dai* ______ **3696 – 3717**

Mesoporous Carbon Materials: Synthesis and Modification

Communications

Glowing after a sugar rush: A molecular switch is formed by inserting glucose-binding protein (GBP) into aequorin (AEQ; see picture). This switch is triggered by recognition of glucose by the GBP. For the first time, AEQ is rationally split into two fragments that, upon a molecular recognition event, come together and emit bioluminescence.

Biotechnology

K. Teasley Hamorsky, C. M. Ensor, Y. Wei, S. Daunert* ______ **3718 – 3721**

A Bioluminescent Molecular Switch For Glucose

Combine and conquer: Configurational assignment of remote stereogenic centers in the complex polyketide macrolide archazolide A (see structure; red O, blue N, yellow S) was accomplished by a purely NMR-based approach relying on a combination of nuclear Overhauser effects, *J* couplings, and residual dipolar couplings (RDCs).

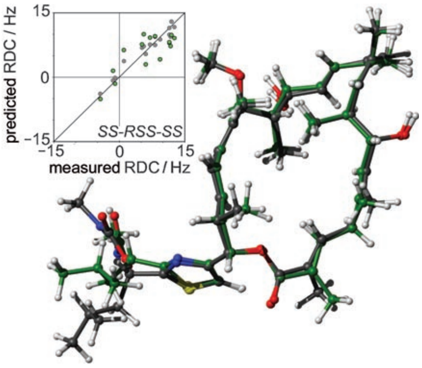

Polyketide Macrolides

C. Farès, J. Hassfeld, D. Menche, T. Carlomagno* ______ **3722 – 3726**

Simultaneous Determination of the Conformation and Relative Configuration of Archazolide A by Using Nuclear Overhauser Effects, *J* Couplings, and Residual Dipolar Couplings

---

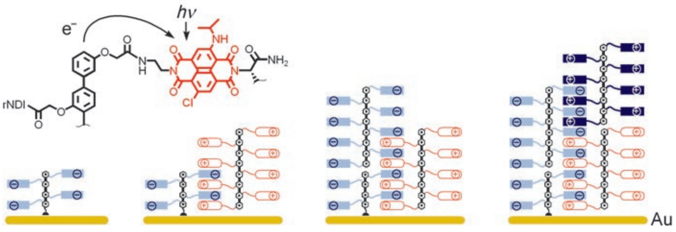

Zipped up: Supramolecular 3D organization on gold with interdigitating intra- and interlayer recognition motifs (see picure, black *p*-oligophenyl rods; red, blue naphthalenediimide (NDI) stacks) is designed to access supramolecular cascade n/p-heterojunctions or the adaptable directionality needed to control fill factors in current–voltage curves.

Artificial Photosynthesis

A. L. Sisson, N. Sakai, N. Banerji, A. Fürstenberg, E. Vauthey,* S. Matile* ______ **3727 – 3729**

Zipper Assembly of Vectorial Rigid-Rod π-Stack Architectures with Red and Blue Naphthalenediimides: Toward Supramolecular Cascade n/p-Heterojunctions

Water-Soluble Nanocrystals

H. Wu, H. Zhu, J. Zhuang, S. Yang, C. Liu, Y. C. Cao* ______ 3730–3734

Water-Soluble Nanocrystals Through Dual-Interaction Ligands

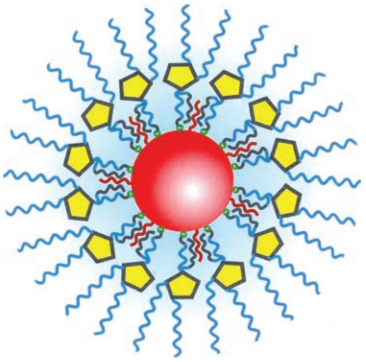

No fear of water: Hydrophobic nanocrystals (NCs) are converted into hydrophilic ones by dual-interaction ligands, which bind onto the surface of NCs by coordinate bonding and hydrophobic van der Waals interactions. The resulting NCs have high stability in aqueous solutions over a wide pH range (1–14), salt concentrations, and thermal treatments. Quantum dots coated with these ligands are excellent fluorescence labels for immunostaining tests.

Luminescent Probes

D.-L. Ma, W.-L. Wong, W.-H. Chung, F.-Y. Chan, P.-K. So, T.-S. Lai, Z.-Y. Zhou, Y.-C. Leung, K.-Y. Wong* ______ 3735–3739

A Highly Selective Luminescent Switch-On Probe for Histidine/Histidine-Rich Proteins and Its Application in Protein Staining

No destaining required: The luminescence properties of an iridium(III)–2-phenylpyridine complex can be utilized for the detection of proteins in sodium dodecyl sulfate–polyacrylamide gels. Emissive gel images obtained upon staining with the complex are visible under UV light. The high detection sensitivity for histidine-rich proteins (right vial, compared to a non-histidine-tagged protein) suggests potential applications in the signaling of biomolecules.

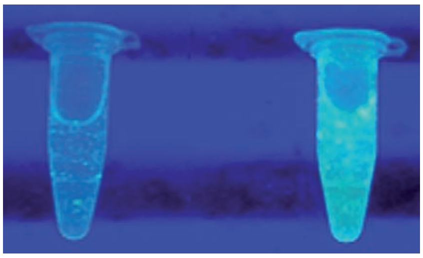

Molecular Recognition

H. Juwarker, J. M. Lenhardt, D. M. Pham, S. L. Craig* ______ 3740–3743

1,2,3-Triazole $CH\cdots Cl^-$ Contacts Guide Anion Binding and Concomitant Folding in 1,4-Diaryl Triazole Oligomers

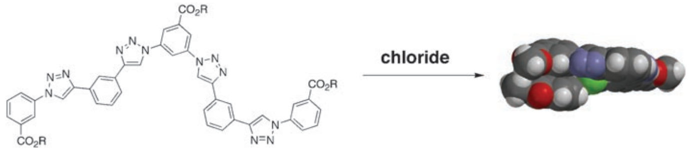

A new folder: The electropositive CH groups of diaryl triazoles interact favourably with chloride, leading to anion-induced helical folding in aryl triazole oligomers. Triazoles thus provide an alternative to conventional protic hydrogen bonds and coordination complexes as functional components in anion receptors.

Embryogenesis

P. Neveu, I. Aujard, C. Benbrahim, T. Le Saux, J.-F. Allemand, S. Vriz, D. Bensimon, L. Jullien* ______ 3744–3746

A Caged Retinoic Acid for One- and Two-Photon Excitation in Zebrafish Embryos

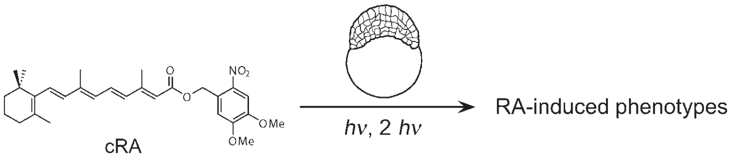

Escaping the cage: Retinoic acid (RA), a crucial signaling molecule for the embryogenesis of vertebrates, can be photoreleased from a simple caged derivative (cRA) upon illumination. In zebrafish embryos, cRA causes RA-induced phenotypes with one- and two-photon excitation (see picture), which opens a route to the noninvasive generation of controlled RA concentration patterns in vivo.

Enzyme Inhibitors

Z. Guo, Y.-W. Wu, K.-T. Tan, R. S. Bon, E. Guiu-Rozas, C. Delon, U. T. Nguyen, S. Wetzel, S. Arndt, R. S. Goody, W. Blankenfeldt, K. Alexandrov,* H. Waldmann* ________ **3747 – 3750**

Development of Selective RabGGTase Inhibitors and Crystal Structure of a RabGGTase–Inhibitor Complex

Stopping the transfer: Based on the structure of pepticinnamin E, specific inhibitors of Rab geranylgeranyl transferase (RabGGTase) with activity in cells were developed, and the first crystal structure of the enzyme in complex with an inhibitor is reported (see inhibitor structure and positioning in the active site of the enzyme). The findings may have implications for the chemical-biological study of Rab prenylation and vesicular transport and the involvement of RabGGTase in the establishment of disease.

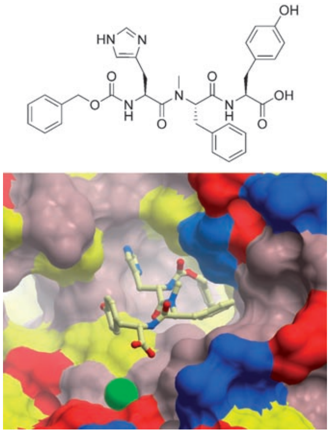

Protein–Polymer Hybrids

A. P. Esser-Kahn, M. B. Francis* ________ **3751 – 3754**

Protein-Cross-Linked Polymeric Materials through Site-Selective Bioconjugation

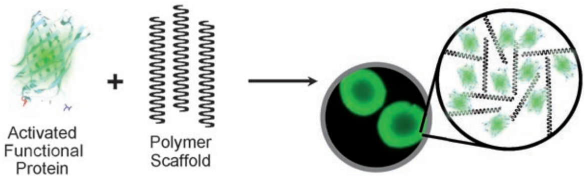

Creating a greener future: A strategy for creating hybrid materials of polymers and proteins relies on orthogonal reactions to activate the N and C termini of a protein concurrently. The protein is then used to cross-link polymer chains and create a hydrogel (see picture). A model hybrid hydrogel containing enhanced green fluorescent protein is both biodegradable and responsive to changes in pH and temperature.

Kinetic Resolution

A. T. Radosevich, V. S. Chan, H.-W. Shih, F. D. Toste* ________ **3755 – 3758**

Synthesis of (−)-Octalactin A by a Strategic Vanadium-Catalyzed Oxidative Kinetic Resolution

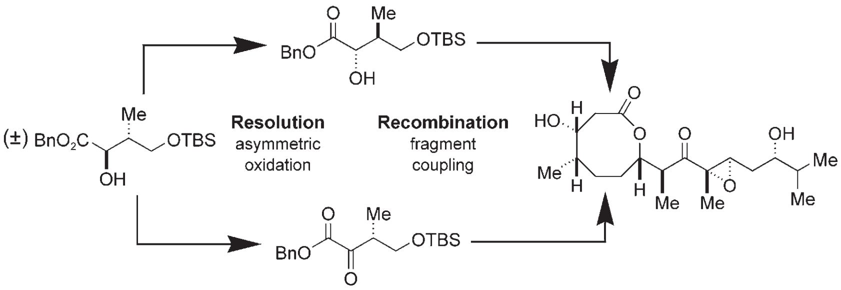

Both products of the kinetic resolution were used in the resolution/recombination approach shown in the scheme for the enantioselective total synthesis of (−)-octalactin A. Bn = benzyl, TBS = *tert*-butyldimethylsilyl.

Drug Synthesis

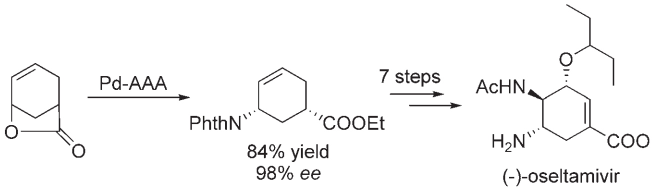

Tackling the supply problem: A short and efficient synthesis of (−)-oseltamivir has been developed which requires eight steps from commercially available starting material and proceeds with an overall yield of 30%. Key transformations include a novel palladium-catalyzed asymmetric allylic alkylation reaction (Pd-AAA, see scheme) as well as a chemo-, regio-, and stereoselective aziridination reaction. Phth = phthaloyl.

Natural Product Synthesis

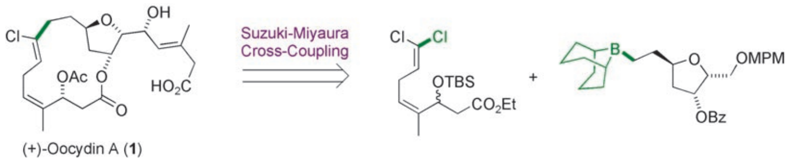

Two sensitive fragments were coupled in the mild title reaction to create the *Z*-chlorovinyl functionality of the target macrolide oocydin A (**1**; see scheme). Another highlight in the total synthesis of **1** was an efficient stereoselective Pd^0-catalyzed cyclization to form the highly substituted tetrahydrofuran ring. Bz = benzoyl, TBS = *tert*-butyldimethylsilyl, MPM = 4-methoxyphenylmethyl.

P_4 Activation

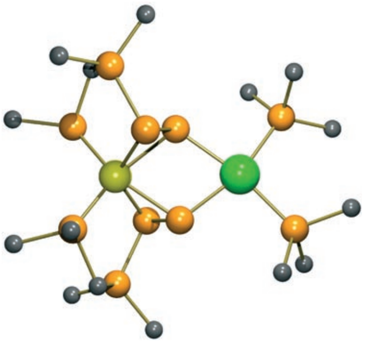

White phosphorus is sequentially activated and functionalized by stepwise reaction with cobalt and platinum metal complexes. The two zwitterionic diphenyl(alkyl)phosphonium(+)diphosphenide(−) molecules generated act as bridging side-on/end-on ligands that tether two different metal units (see picture of the complex core: C black, Co pale green, P orange, Pt green).

Vanadium(V) Alkylidenes

Honeycomb architectures from N_2 sequestration! The V^{III}–bis-neopentyl complex $[(PNP)V(CH_2tBu)_2]$ (PNP = $N[4\text{-}Me\text{-}2\text{-}(PiPr_2)C_6H_3]_2^-$) is a synthon to terminal V^V alkylidene complexes when treated with two-electron oxidants such as N_2CPh_2, O^{2-} sources such as $OPPh_3$ and N_2O, and sulfide sources like S_8 and $SPPh_3$. The likely V^{III}–alkylidene intermediate, $[(PNP)V{=}CHtBu]$, can also activate N_2 to form a honeycomb-like packing rearrangement along the N_2 unit (see picture).

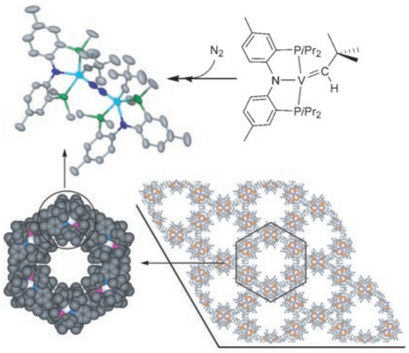

Contents

Antitumor Agents

B. Therrien,* G. Süss-Fink,
P. Govindaswamy, A. K. Renfrew,
P. J. Dyson ______ **3773 – 3776**

The “Complex-in-a-Complex” Cations $[(acac)_2M\subset Ru_6(p\text{-}iPrC_6H_4Me)_6(tpt)_2(dhbq)_3]^{6+}$: A Trojan Horse for Cancer Cells

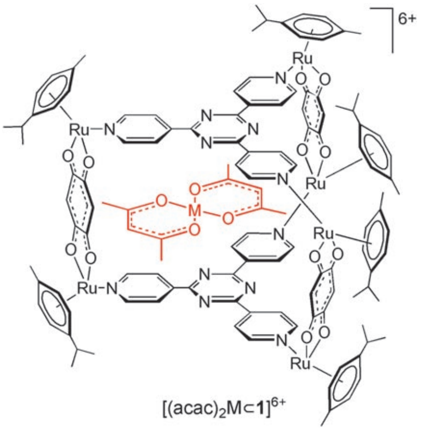

The start of an odyssey? The cytotoxicities of the large cationic arene–ruthenium prismatic cage $\mathbf{1}^{6+}$, and its “complex-in-a-complex” derivatives $[(acac)_2M\subset\mathbf{1}]^{6+}$ (M = Pd, Pt; acac = acetylacetonate; see picture), are evaluated in comparison with free $[M(acac)_2]$. The differences in cytotoxicity suggest that, like a “Trojan Horse”, leaching of the guest from the cage once inside a cell accelerates and increases the cytotoxic effect.

Asymmetric Catalysis

R. J. Detz, M. M. E. Delville, H. Hiemstra,
J. H. van Maarseveen* ______ **3777 – 3780**

Enantioselective Copper-Catalyzed Propargylic Amination

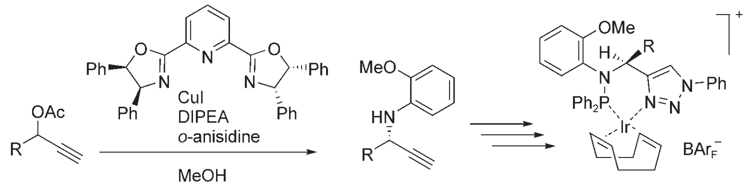

A proper copper catalyst with a chiral pyridine-2,6-bisoxazoline (pybox) ligand was used to convert a variety of propargylic acetates with aromatic side chains (R = Ar) into their amine counterparts in high yield and with good selectivity (up to 88 % *ee*). The resulting chiral propargylic amines can be elaborated further into P,N ligands (see scheme; DIPEA = diisopropylethylamine).

Asymmetric Amination

G. Hattori, H. Matsuzawa, Y. Miyake,
Y. Nishibayashi* ______ **3781 – 3783**

Copper-Catalyzed Asymmetric Propargylic Substitution Reactions of Propargylic Acetates with Amines

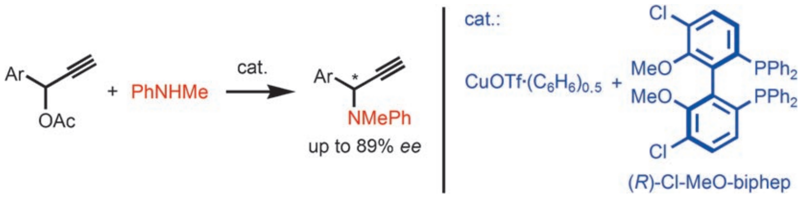

Flexing your bipheps: Enantioselective propargylic substitution reactions of propargylic acetates with amines catalyzed by a copper-(*R*)-Cl-MeO-biphep or -binap complex give the corresponding propargylic amines in excellent yields with up to 89 % *ee*. The reaction described may provide a novel synthetic method for the preparation of chiral propargylic amines.

Nitrogen Heterocycles

M. Yar, E. M. McGarrigle,
V. K. Aggarwal* ______ **3784 – 3786**

An Annulation Reaction for the Synthesis of Morpholines, Thiomorpholines, and Piperazines from β-Heteroatom Amino Compounds and Vinyl Sulfonium Salts

Heterocycling: Diphenyl vinyl sulfonium salt **1** acts first as an electrophile, then a base, and then again as an electrophile in this operationally simple, high yielding, one-pot synthesis of pharmacologically important morpholines, thiomorpholines, and piperazines. Compound **1** is an excellent synthon for the 1,2-ethane dication.

Oxidation

T. Dohi, A. Maruyama, N. Takenaga,
K. Senami, Y. Minamitsuji, H. Fujioka,
S. B. Caemmerer, Y. Kita* ____ **3787 – 3790**

A Chiral Hypervalent Iodine(III) Reagent for Enantioselective Dearomatization of Phenols

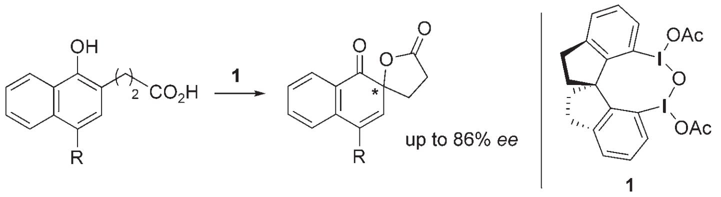

The hype about iodine(III): A chiral hypervalent iodine(III) reagent (**1**) is reported to enantioselectively dearomatize phenols in a highly selective manner (see scheme). This result clearly supports existence of the associative pathway in hypervalent iodine(III)-induced phenolic oxidations.

Noncentrosymmetric Vanadates

W. L. Queen, J. P. West, S.-J. Hwu,*
D. G. VanDerveer, M. C. Zarzyczny,
R. A. Pavlick ____ **3791 – 3794**

The Versatile Chemistry and Noncentrosymmetric Crystal Structures of Salt-Inclusion Vanadate Hybrids

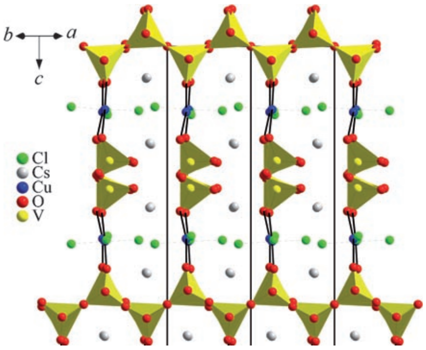

Acentric vanadates: Three unique structure types of the vanadate-based mixed-metal oxide systems (salt)·Mn^{II}-V^{V}-O and (salt)·Cu^{II}-V^{V}-O are presented, with a focus on the role of the asymmetric vanadate units (yellow polyhedra). The two structure types found in the $(AX)_2M(VO_3)_2$ series differ in the propagation direction of the metavanadate chains, which is thought to be due to the presence (or absence) of a Jahn–Teller distortion of the metal (d^9 Cu^{2+} vs. d^5 Mn^{2+}) ion.

Asymmetric Catalysis

M. Kawasaki, P. Li,
H. Yamamoto* ____ **3795 – 3797**

Enantioselective O-Nitroso Aldol Reaction of Silyl Enol Ethers

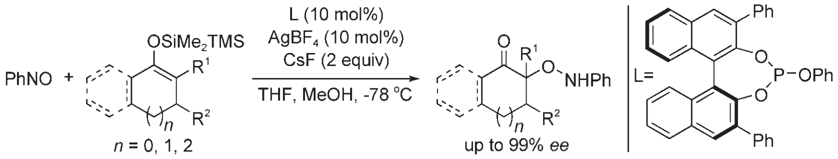

New nucleophiles for the O-nitroso aldol reaction in the form of readily prepared disilanyl enol ethers make this transformation more practical and more versatile. A silver catalyst with a chiral biaryl phosphite ligand promotes the title reaction with high enantio- and regioselectivity (see scheme). R^1,R^2 = H, Ar; TMS = trimethylsilyl.

Electron Transfer

F. D. Lewis,* P. Daublain, B. Cohen,
J. Vura-Weis,
M. R. Wasielewski* ____ **3798 – 3800**

The Influence of Guanine on DNA Hole Transport Efficiency

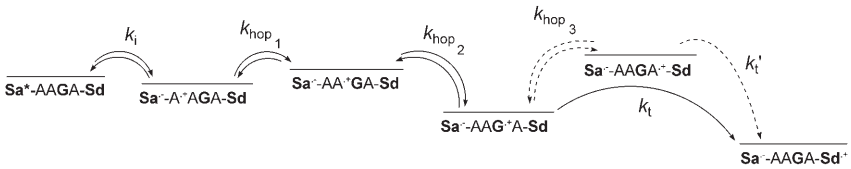

Stopover at G base: The efficiency of photoinduced charge separation between donor and acceptor chromophores separated by a polyadenine sequence containing a single guanine (G) is sensitive to the location of G and the total length of the polypurine sequence. Quantum yields provide support for a stepwise mechanism in which G serves as a temporary resting place in the overall process (Sa: stilbenedicarboxamide electron acceptor, Sd: stilbenediether electron donor).

P versus C Protonation

Y. Zhang, F. S. Tham, J. F. Nixon, C. Taylor,
J. C. Green, C. A. Reed* ____ **3801 – 3804**

The Low Basicity of Phosphabenzenes: First Examples of Protonation, Alkylation, and Silylation Reactions

Strong yet gentle: Where triflate reagents fail, carborane-based sources of H^+, CH_3^+, and $[R_3Si]^+$ electrophiles add to phosphabenzenes preferentially at the P atom rather than C (see picture).

Gold Catalysis

X.-Y. Liu, C.-M. Che* ______ **3805 – 3810**

A Highly Efficient and Selective Au^I-Catalyzed Tandem Synthesis of Diversely Substituted Pyrrolo[1,2-*a*]quinolines in Aqueous Media

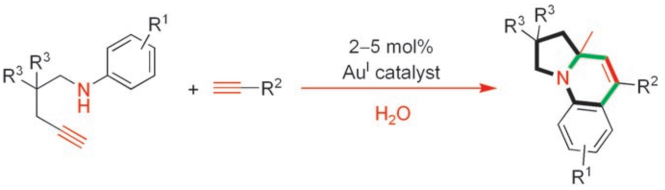

Bicycles built in water: The Au^I-catalyzed tandem cyclization of 1-amino-4-alkynes with alkynes in water offers a simple and efficient method for the synthesis of diversely substituted pyrrolo[1,2-*a*]quinolines with good to excellent product yields and excellent regio- and chemoselectivities (see scheme).

Sensors

T. Rantanen,* M.-L. Järvenpää, J. Vuojola,
K. Kuningas, T. Soukka ____ **3811 – 3813**

Fluorescence-Quenching-Based Enzyme-Activity Assay by Using Photon Upconversion

Switch the lights off! A novel sensitive enzyme-activity assay combines the advantageous features of upconverting phosphors (UCPs) and fluorescence quenching. The new assay principle allows the use of fluorescent particulate labels in a quenching-based assay despite the fact that it is not possible to achieve adequate quenching efficiency of particle fluorescence directly. Infrared excitation enables even the use of colorful samples.

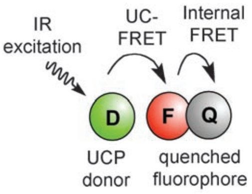

Nanostructures

L. Cademartiri, R. Malakooti,
P. G. O'Brien, A. Migliori, S. Petrov,
N. P. Kherani, G. A. Ozin* _ **3814 – 3817**

Large-Scale Synthesis of Ultrathin Bi_2S_3 Necklace Nanowires

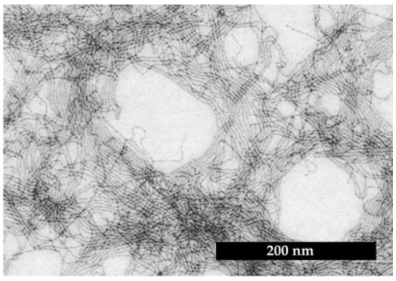

Think thin! Colloidally stable ultrathin Bi_2S_3 nanowires (see picture), which display strong excitonic features never before seen in bismuth chalcogenides and extremely high extinction coefficients, have been synthesized on a gram-scale. Nanostructures such as this are of very high technological potential for thermoelectric applications.

Asymmetric Catalysis

C. Walter, M. Oestreich* ___ **3818 – 3820**

Catalytic Asymmetric C–Si Bond Formation to Acyclic α,β-Unsaturated Acceptors by Rh^I-Catalyzed Conjugate Silyl Transfer Using a Si–B Linkage

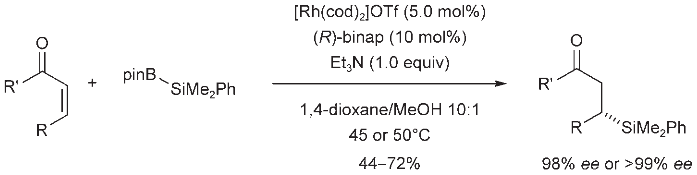

A perfect match: The Rh^I-catalyzed conjugate silylation of acyclic *Z*-configured α,β-unsaturated carboxyl compounds including imides with silylboronic ester yields almost enantiopure α-chiral quaternary silanes (see scheme; R = aryl and (branched) alkyl, cod = cycloocta-1,5-diene, pin = pinacolato).

Host–Guest Chemistry

C. Meier, K. Landfester, D. Künzel,
T. Markert, A. Groß,
U. Ziener* ———— 3821 – 3825

Hierarchically Self-Assembled Host–Guest Network at the Solid–Liquid Interface for Single-Molecule Manipulation

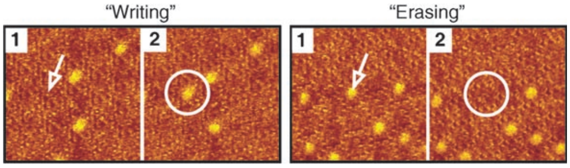

Now you see it, now you don't: A molecular monolayer polymorph of an oligopyridine forms a host–guest network with copper(II) phthalocyanine at the solid–liquid interface with controllable phthalocyanine occupation. The slow movement of the phthalocyanine guest molecules and the competition between oligopyridine and phthalocyanine guest molecules make it possible to manipulate individual guest molecules in analogy to "writing" and "erasing".

Ansa Complexes

VIP

H. Braunschweig,* C. J. Adams, T. Kupfer,
I. Manners, R. M. Richardson,
G. R. Whittell ———— 3826 – 3829

Synthesis of a Paramagnetic Polymer by Ring-Opening Polymerization of a Strained [1]Vanadoarenophane

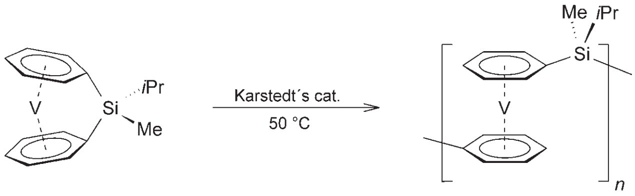

Salt-elimination reactions led to the formation of highly strained [1]bora- and [1]silavanadoarenophanes, which undergo different types of ring-opening reactions with low-valent platinum complexes. Whereas the boron-bridged derivative opened stoichiometrically by cleavage of the V–C_{arene} bond, the [1]silavanadoarenophane reacted at the Si–C_{ipso} bond to afford a polymer containing spin-active metal centers in the main chain (see scheme).

Ionic Liquids

K. Fumino, A. Wulf,
R. Ludwig* ———— 3830 – 3834

The Cation–Anion Interaction in Ionic Liquids Probed by Far-Infrared Spectroscopy

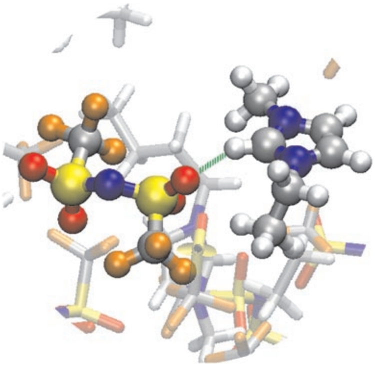

Bending and stretching: The nature of intermolecular interactions in imidazolium-based ionic liquids has been studied by far-infrared spectroscopy. The lowest frequencies can be assigned to the bending and stretching vibrational modes of the cation–anion interaction, which describes the cohesion energy.

Supporting information is available on www.angewandte.org (see article for access details).

A video clip is available as Supporting Information on www.angewandte.org (see article for access details).

Contents

Service

Corrigendum

Ferrocenyl Ligands with Two Phosphanyl Substituents in the α,ε Positions for the Transition Metal Catalyzed Asymmetric Hydrogenation of Functionalized Double Bonds

T. Ireland, G. Grossheimann, C. Wieser-Jeunesse, P. Knochel ______ **3212–3215**

Angew. Chem. Int. Ed. **1999**, *38*

DOI 10.1002/(SICI)1521-3773(19991102)38:21<3212::AID-ANIE3212>3.0.CO;2-9

Following a remark by Fukuzawa et al.,[1] we confirm that the stereochemistry of ferrocenyl ligands **2** is not (R,S_{Fc}) as described in the original communication, but (R,R_{Fc}) as indicated by the X-ray structure of the [Rh(nbd)(**2a**)]BF_4 complex included in the manuscript. Thus, the ferrocene derivatives **2a** and **2b** have (R,R_{Fc}) configuration (Scheme 1).

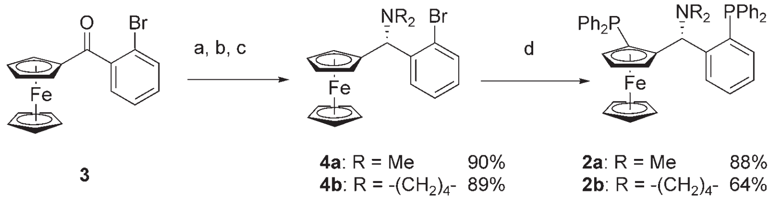

Scheme 1. a) CBS catalyst (0.3 equiv), BH_3–Me_2S, 0 °C, 2 h; b) Ac_2O, pyridine, 12 h; c) HNR_2, CH_3CN, H_2O, 12 h; d) *t*BuLi (3.5 equiv), −78 °C to room temperature (RT), 1 h; then $ClPPh_2$ (2.5 equiv), −78 °C to RT, 1 h.

---

[1] S. Fukuzawa, M. Yamamoto, M. Hosaka, S. Kikuchi, *Eur. J. Org. Chem.* **2007**, 5540.